Supplementary information

Unraveling the relationship between Sr stoichiometry in $Sr_xFe_{1.5}Mo_{0.5}O_{6-\sigma}$ and its catalytic performance for high-temperature CO_2 electrolysis

Xiuan Xi[a], Xiaoyu Liu[a], Lingui Huang[a], Jianwen Liu[a], Bo-Wen Zhang[b], Gadi Rothenberg[c], Xian-Zhu Fu[a, *], Jing-Li Luo[a, *]

[a] *College of Materials Science and Engineering, Shenzhen University, Shenzhen 518060, China*

[b] *Department of Chemical and Materials Engineering, University of Alberta, Edmonton, AB T6G 1H9, Canada*

[c] *Van 't Hoff Institute for Molecular Sciences, University of Amsterdam, Science Park 904, 1098XH Amsterdam, The Netherlands*

* Corresponding authors

E-mail addresses: xz.fu@szu.edu.cn (X.-Z. Fu); jingli.luo@ualberta.ca (J.-L. Luo)

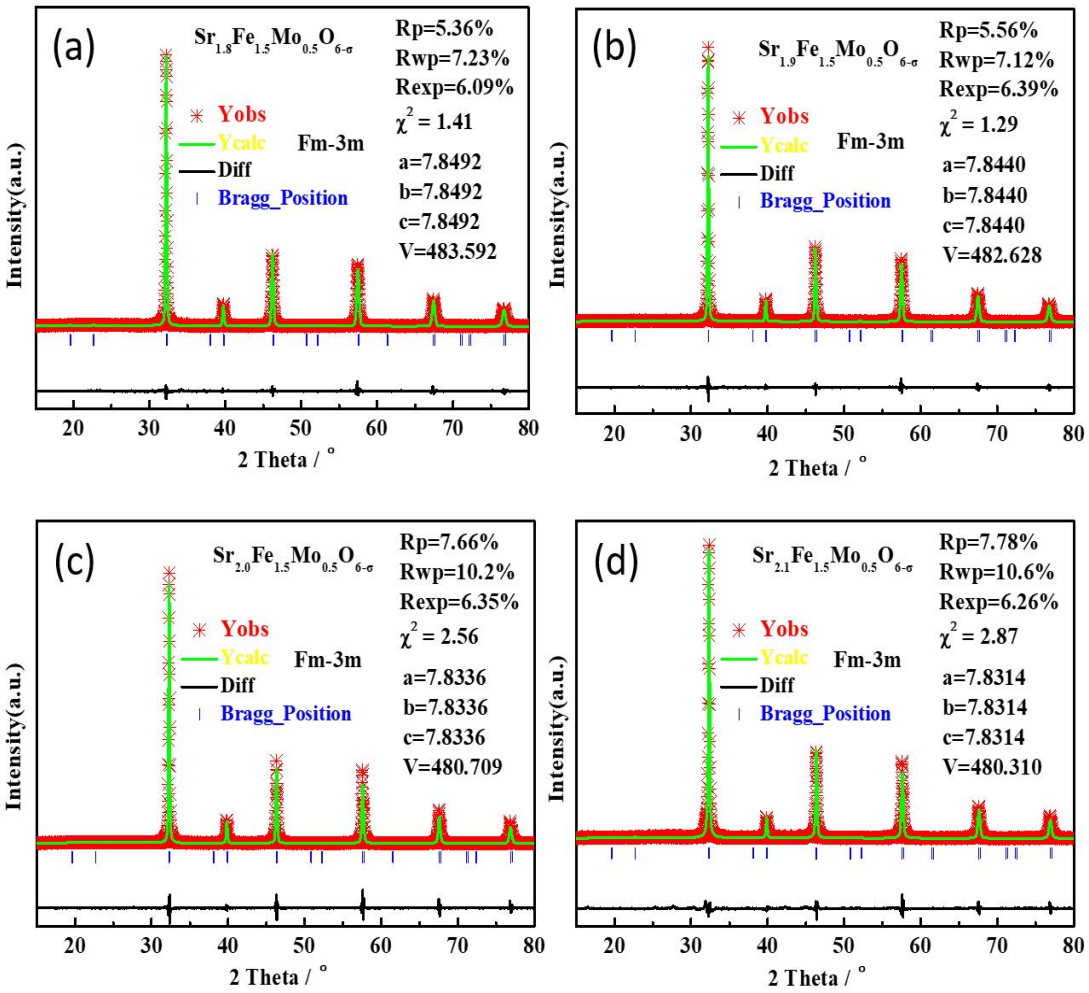

Fig. S1. Refined XRD patterns of the as-prepared $Sr_xFe_{1.5}Mo_{0.5}O_{6-\sigma}$ powders: (a) $Sr_{1.8}Fe_{1.5}Mo_{0.5}O_{6-\sigma}$, (b) $Sr_{1.9}Fe_{1.5}Mo_{0.5}O_{6-\sigma}$, (c) $Sr_{2.0}Fe_{1.5}Mo_{0.5}O_{6-\sigma}$, (d) $Sr_{2.1}Fe_{1.5}Mo_{0.5}O_{6-\sigma}$.

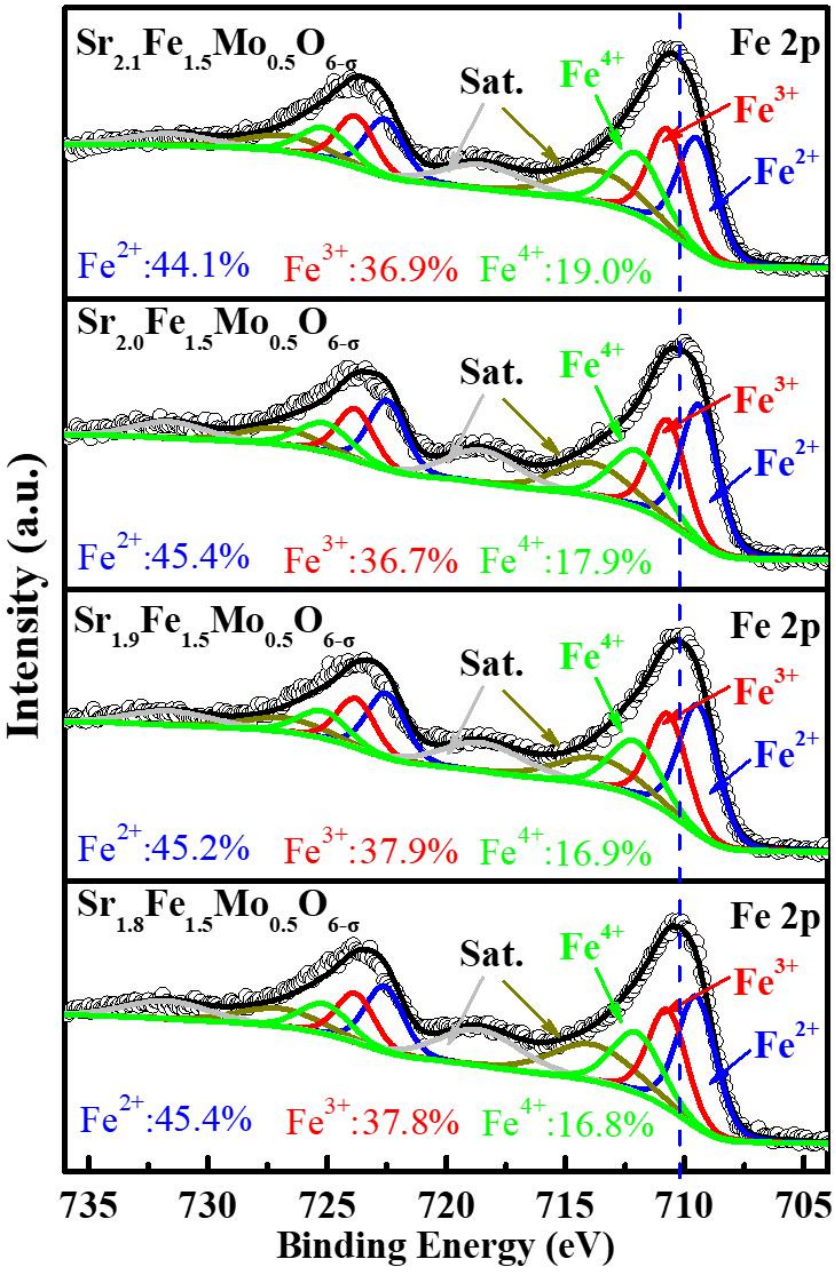

Fig. S2. XPS Fe 2p spectra of the $Sr_xFe_{1.5}Mo_{0.5}O_{6-\sigma}$ samples.

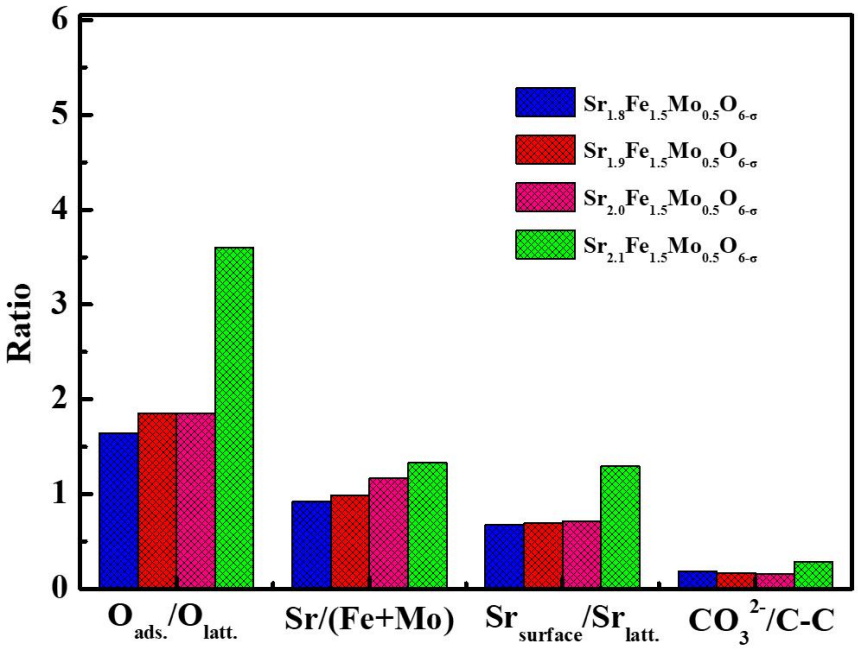

Fig. S3. Ratio change of the $O_{ads.}/O_{latt.}$, Sr/(Fe+Mo), $Sr_{surface}/Sr_{latt.}$, and CO_3^{2-}/C-C.

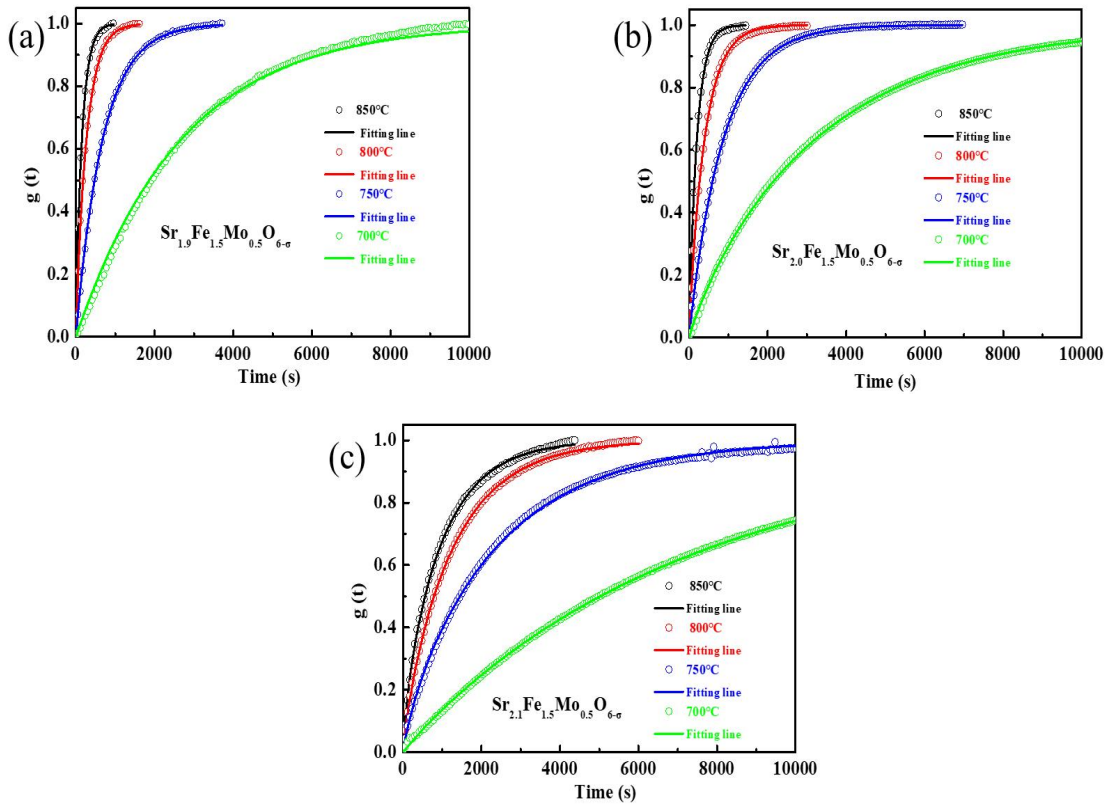

Fig. S4. Electrical conductivity relaxation (ECR) results of the different samples at the different operating temperature.

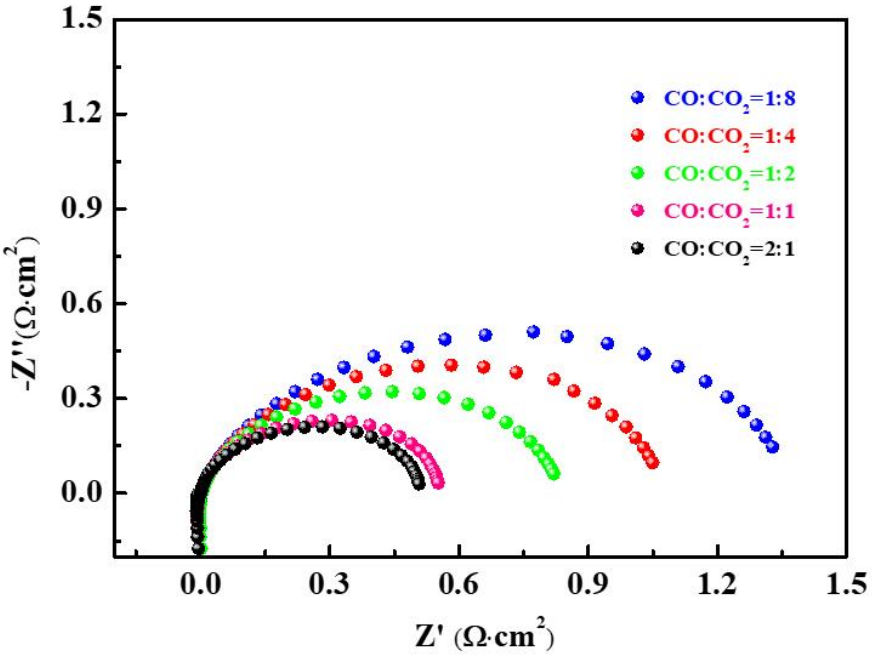

Fig. S5. EIS results of the $Sr_{1.9}Fe_{1.5}Mo_{0.5}O_{6-\sigma}$ samples under different oxygen partial pressures at the operating temperature of 800 °C.

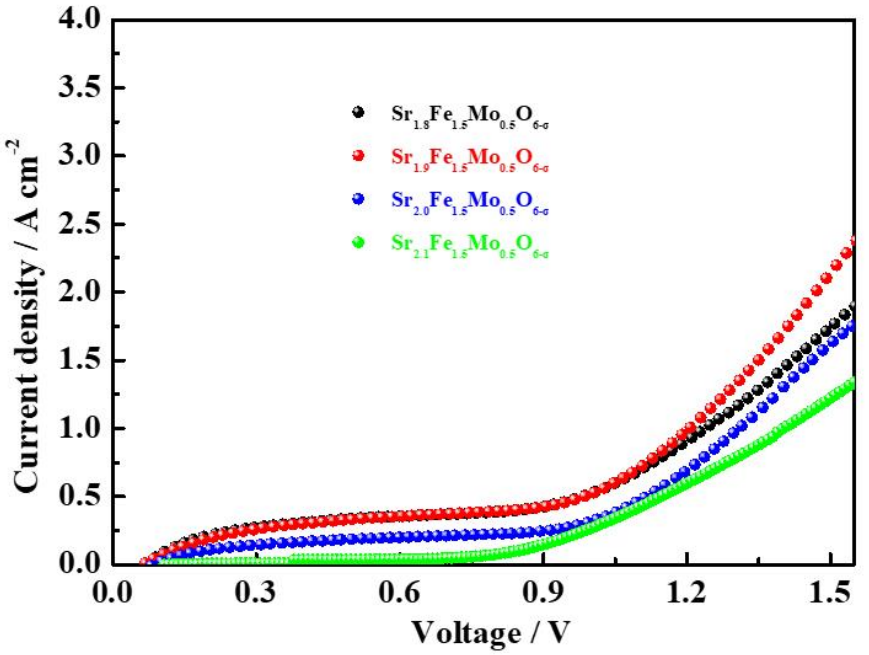

Fig. S6. Current density of the single cell with different cathode materials under a pure CO_2 atmosphere and different applied potentials (800 °C).

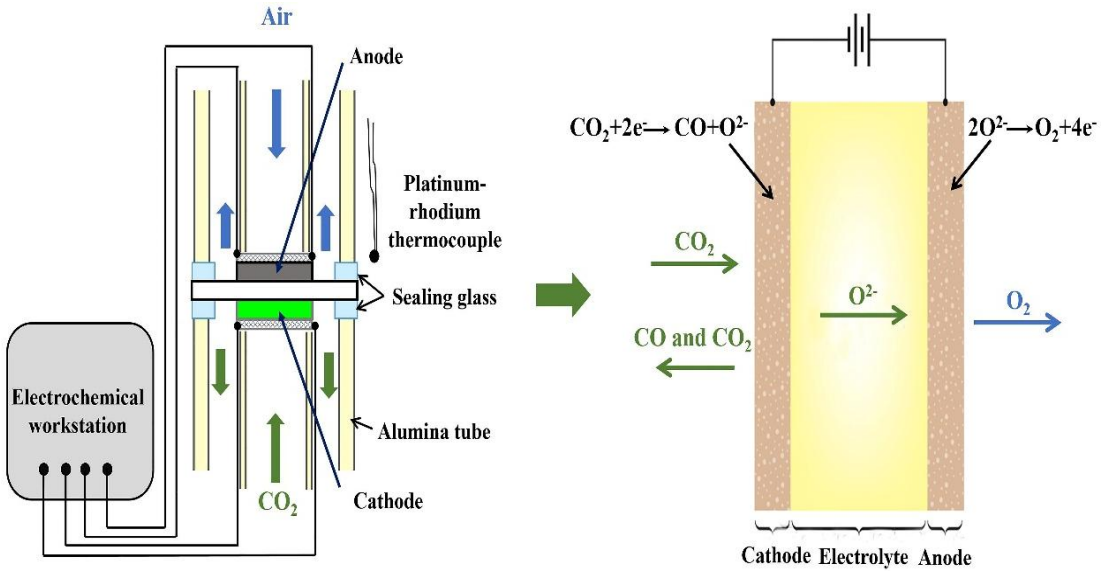

Fig. S7. Schematic diagram of the cell configurations for electrochemical performance testing